7-2021

A Time-course Characterization of Muscle Function and Mitochondrial Markers During Colorectal Cancer-induced Cachexia in Tumor-bearing Male Mice

Ana Cabrera Ayuso
University of Arkansas, Fayetteville

A Time-course Characterization of Muscle Function and Mitochondrial Markers During Colorectal Cancer-induced Cachexia in Tumor-bearing Male Mice

A thesis submitted in partial fulfillment
of the requirements for the degree of
Master of Science in Cell and Molecular Biology

by

Ana Cabrera Ayuso
University of San Carlos of Guatemala
Licentiate Degree in Chemical Biology 2011

July 2021
University of Arkansas

This thesis is approved for recommendation to the Graduate Council.

_____
Nicholas P. Greene, Ph.D
Thesis Director

_____
Tyrone A. Washington, Ph.D
Committee Member

_____
Timothy J. Muldoon, Ph.D
Committee Member

Abstract

Cachexia is a multisystemic and multifactorial syndrome prevalent in cancer patients. It is clinically defined by involuntary loss of >5% weight in a six-month window, despite nutritional interventions. A negative energy balance characterizes cancer cachexia (CC), it is associated with weakness and fatigue in skeletal muscle. Impaired muscle function is associated with lower quality of life in cancer patients. Defects in mitochondrial function are strongly associated with muscle wasting. This study explored muscular contractile function and mitochondrial quality control (MQC) markers in soleus, gastrocnemius, and tibialis anterior (TA) muscles of C26-induced male tumor-bearing mice during a 25-day time course. It was demonstrated that C26 colorectal cancer induces skeletal muscle atrophy aggravated as it develops, with a reduction up to 15% in body weight, affecting all the mentioned tissues. Higher fatigue is present after 25 days of tumor development, and an overall decrease in the isometric force could be seen starting after 10 days. *Opa1*, *Fis1*, *Bnip3*, *Lonp1*, and *Parl1* mRNA content was measured in the three tissues, with a lower content of *Opa1* in TA and a greater increased *Bnip3* content on gastrocnemius after 25 days. No significant differences were observed in *Fis1*, *Lonp1*, or *Parl1* 25 days following tumor allograft compared to PBS control. In conclusion, this study showed the induction of CC by C26 colon carcinoma, associated with a decrease in muscle force and higher fatigue with intrinsic differences in the mitochondrial metabolism and heterogenicity of different muscle responses to CC in males.

Acknowledgment

I want to thank:

To the Fulbright-LASPAU scholarship, which allowed me to study in a first-line university like UARK, live new experiences, and get to know so many cultures.

To the Universidad de San Carlos de Guatemala – USAC, for support me and believe in me as an agent of change for my country, especially to my Biochemistry Department colleagues for encouraging me to pursue a higher academic degree and never settled down.

To the National Institute of Arthritis and Musculoskeletal and Skin Diseases of the National Institute of Health (NIH) for the funding to do this project because science is never cheap.

To Dr. Nicholas Greene for adopting me into his lab family and belief in women doing science. Thank you for all the effort and extra work you have done for this (and more) to happen, and of course, for making science cool.

To my thesis committee members Dr. Tyrone Washington and Dr. Timothy Muldoon, I highly value your guidance through this time-limited learning process. Especially for being open-minded and supportive when science is not going as expected (I guess it never does).

To the members of the Cellular Energetics and Mitochondrial Disorders Laboratory.

To the members of the Exercise Muscle Biology Laboratory and the Cachexia Research Laboratory, for being the geekiest and coolest lab members, especially Fran and Seong, for being more than just exceptional lab mates in my life.

To all faculty, staff, and students of the Exercise Science Research Center.

To all the Fulbright community and extended friends in Fayetteville, specially Harumi, for being my CEMB partner in crime and Osnar for being my support and emotional strength.

To all my friends in Guate for share the losses and celebrate the wins even from far.

And finally, but mostly to my family, I love you, and I miss you. Thanks for being so close while being far.

Table of Contents

List of Tables

List of Figures

1. Introduction

Cachexia is a multisystemic and multifactorial syndrome prevalent in cancer patients[1,2]. It is clinically defined by the involuntary loss of >5% weight in a six-month window, persisting after nutritional interventions[1,3-5]. Cancer cachexia (CC) is characterized by a negative energy balance[6], with skeletal and cardiac muscle the major affected tissues[5]. The mass loss can occur with or without loss of fat mass[7,8]. Skeletal muscle represents 40-50% of total body weight[5] and, therefore, plays crucial physical and metabolic roles in humans[9]. Muscle has extraordinary metabolic plasticity, allowing it to respond to different environmental conditions[10] such as protein availability, energy demands, the force needed for body movement, among others[9]. During CC, muscle mass and fibers diameter are controlled by the protein turnover[7,11], myofiber remodeling, flawed muscle mitochondrial activity, and other factors[7,9]. Failure to adapt these metabolic processes displaces homeostasis between anabolism and catabolism of myotubular proteins, leading to muscle wasting[12-14].

Atrophy is closely associated with muscle weakness and fatigue[15]. Muscle weakness can be attributed to muscle wasting mass, menacing muscle function[16,17]. Muscular dysfunction and loss of muscle mass are clinical trademarks of CC[16]. It can serve as a predictor of survival due to impaired muscle function is strongly associated with a lower survival rate and quality of life in cancer patients[18-20]. According to Tisdale and coworkers[13], lower protein concentration, smaller fibers, decreased force production, and fatigue resistance are common features in cancer-induced skeletal muscle atrophies. Moreover, fatigue is a common symptom reported in cancer patients with cachexia[18]; it is attained when muscle failures to preserve force[16], although the underlying mechanism of how CC drives fatigue is still unknown[16].

There is a solid relationship between mitochondrial fitness and muscle health[6,21]. Faulty mitochondria have been emerged as an important regulator of muscle wasting[9]. Recent publications have linked mitochondria' impairment with tissue metabolic imbalance during the beginning of cachexia, affecting muscle size and quality[1,6,22]. Skeletal muscle mitochondria help to supply muscle contractions with high ATP demands through oxidative phosphorylation (OXPHOS)[14]. Mitochondria is a multifunctional organelle. They are involved in calcium signaling, reactive oxygen species (ROS) emission, inflammation, ammonia detoxification, substrate metabolism, cofactors, cell differentiation, apoptosis, and autophagy[7,23-26]. Changes in mitochondrial content, shape, or function are imperative to maintain muscle plasticity[27], healthfulness, and performance to preserve cellular fitness[7,23,28]. Even so, cellular stress increases mitochondrial damage, and accumulation of mitochondrial damage can lead to diseases or cell death[29]. Because skeletal muscle fibers are post-mitotic, and mitochondria do not originate *de novo*, cellular division cannot dilute any potential damage acquired[23,27]. Therefore, mitochondria rely on different mitochondrial quality control (MQC) mechanisms activated depending on the extent of the damage[7,14,23]. MQC systems include mitochondrial biogenesis, dynamics (fission and fusion), mitochondrial matrix chaperones, intramitochondrial proteases, mitochondrial-derived vesicles, and mitochondrial autophagy (mitophagy)[7,23,29,30]. Mitochondrial dynamics is a very active MQC system consisted of two opposite mechanisms: fission and fusion, the balance between these events will determine its morphology[29], number, quality, and cell distribution[25]. Mitochondrial fission consists of fragmentation and mitophagy promotion[29], and it is required to clear away damaged components[7]. Thus, the network disruption will generate shorter organelles[27] while helping to segregate damaged mitochondria and promoting their removal[18]. Dynamin-related protein 1 (DRP1) and Fission protein 1 (FIS1)

are needed for this mitochondrial division[31]. DRP1 translocates to the outer mitochondrial membrane (OMM) to create active fission sites by binding to FIS1 at the OMM[22,31]. On the contrary, mitochondrial fusion occurs when two or more mitochondria join together, mixing their content and generating more extensive networks and elongated organelles[7,25,27]. This process helps to dilute any potentially damaged elements[23,27] and avoid auto-phagocytosis by increasing mitochondrion size[29]. Fusion of the OMM is regulated by Mitofusin (MFN) 1 and 2; similarly, optic atrophy 1 (OPA1) is responsible for the fusion of the inner mitochondrial membrane (IMM)[23,25]. OPA1 knockdown has been associated with mitochondrial fragmentation[23]. Moreover, disrupted mitochondrial dynamics have been observed in pre-clinical animal model of CC in where protein content of OPA1 was reduced during the development of the disease[1].

Mitochondrion lifespan is 10-25 days[28]. Thus, mitophagy is needed to balance mitochondrial turnover or degrade damaged mitochondria in response to cellular needs[7,24,28,32]. Any disruption in mitophagy can lead to cellular damage or death[32]. Mitophagy can be mediated either by ubiquitination or receptor[24]. BNIP3 (Bcl- 2/adenovirus E1B 19kDa-interacting protein 3) is an OMM receptor involved in mitophagy with an LC3-interaction region (LIR) that facilitates its binding to the autophagosome[9,23,24,32]. Overexpression of BNIP3 is related to increased mitophagy and has been found up-regulated in CC[7,23]. More so, ROS are formed as a byproduct of OXPHOS, exposing mitochondria to strong oxidative stress[33,34]. Cellular stress increases mitochondrial protein damage, leading to proteotoxicity if mitochondrial proteostasis is flawed[26,34,35]. Accumulation of misfolded proteins can lead to dissipation of the mitochondrial membrane potential (MMP), change in mitochondrial shape, and dysfunction[30]. Mitoproteases, as part of the MQC systems, are the first line mitochondrial defenders acting as a surveillance system to maintain a healthy protein turnover inside these organelles[24,27,36]. More than 45

different mitoproteases have been reported in mammals, and they can be classified as transient or resident, depending on where they are localized[24]. Lon peptidase 1 (LONP1) is the most abundant soluble mitochondrial matrix (MM) ATP-dependent protease[36-38]. It is broadly expressed in high-energy consuming tissues, such as heart, brain, liver, and skeletal muscle[34]. These mitoproteases have been described as essential components of the MQC machinery[30,34,37]. In mammals, LONP1 knockout is deleterious to life[36]. Its primary function appears to be to degrade misfolded MM proteins [24] and regulate several cellular and metabolic functions[30,33,34,36-38]. Moreover, quality control is also needed in the IMM. Besides LONP1, Rhomboid proteases play an essential role in controlling proteome quality in the IMM[39]. Presenilins-associated rhomboid-like (PARL1) is a membrane-embedded peptidase that cleaves substrates such as PINK1 (PTEN-induced kinase 1) and Smac/Diablo, therefore regulating mitophagy and apoptosis[39]. PARL1 can also regulate mitochondrial morphology through OPA1[25]. OPA1 is an IMM nuclear gene encoding mitochondrial protein (NuGEMP)[23]. It is cleaved after its importation from the nucleus producing a long isoform (L-OPA1)[25]. The L-form will anchor to the IMM where PARL1 will yield the short form (S-OPA1), promoting mitochondria fusion[25]. Failure in PARL activity leads to defects in mitochondrial biogenesis, morphology and function, high apoptosis rate, and atrophy[27,39].

Even though cancer is one of the leading causes of mortality worldwide and the development of CC in patients is among the main causes of death, no effective therapies are yet available. To date, CC remains an untreated condition[4,15]. Thus, it is necessary to further investigate the critical mechanisms of this pathology and how it affects muscle function and identify efficacious therapeutic targets to prevent the induction or evolution of this disease. Hence, the present study was performed using tumor-bearing male mice during a 25-day time-course of colorectal cancer-

induced cachexia, contributing to describing the impact of CC on muscle function through isometric torque frequency force and fatigue characterization and mitochondrial markers trend for dynamics, mitophagy, and mitoproteases. Therefore, the purpose of this study was to assess the skeletal muscle function during the time-course of C26-colorectal cancer-induced cachexia in tumor-bearing mice and characterize the alterations of mitochondrial quality control markers on skeletal muscle during the time-course of C26-colorectal cancer-induced cachexia in tumor-bearing male mice.

2. Material and Methods

2.1 Animals and Experimental Design

All experiments were approved by the University of Arkansas Institutional Animal Care & Use Committee. BALB/c male mice were purchased from Jackson Laboratories (Bar Harbor, ME, USA) and housed in a temperature-controlled environment maintained on a 12:12 hours light-dark cycle. The mice received *ad libitum* access to water and chow for the duration of the study. CC was induced by injecting $5X10^5$ C26 colorectal cancer cells bilaterally into each hind flank of eight-weeks old mice for a total of $1X10^6$ cells, or with sterile phosphate buffered saline (PBS) as sham control. Tumors were allowed to develop for 10 days, 15 days, 20 days, or 25 days, PBS treated mice were allowed 25 days from injection to age-match 25 days tumor-bearing mice. Each experimental group consisted of 10-12 animals; total experimental animal numbers: n~ 69.

2.2 C26 Culture and Cancer Injections

C26 colon carcinoma fibroblast (National Cancer Institute) were cultured in 10% Growth Media (10%GM). This media was made with DMEM – Dulbecco's Modified Eagle Medium, high glucose (Gibco, 11965118), supplemented with 1% penicillin/streptomycin, and 10% Fetal Bovine Serum (FBS). Cells were incubated at 37°C and 5% CO_2 until 80-90% confluency. Media was aspired, and cells were washed twice with Phosphate Buffered Saline (PBS). 0.05% Trypsin (25300054, Gibco, USA) was added and incubated at 37°C and 5% CO_2 for 5 minutes. 10%GM was added, and cell solution was spin at 250 rpm for 5 minutes. Supernatant was aspired, and cells were resuspended in 10%GM. Cells were counted using a hemocytometer, and $1x10^6$ cells were suspended in 200 μL of PBS. At eight weeks old, mice were anesthetized with isoflurane in O_2, shaved on the right and left flank, and 100 uL of C26 cells/PBS diluted were injected on each side ($5X10^5$ to each flank for $1X10^6$ total). The control group received an equal volume of sterile PBS. Mice were allowed to be recovered and observed until tissue collection.

2.3 *In Vivo* Assessment of Muscle Function

Forty-eight hours prior to tissue harvest, skeletal muscle contractility (*in vivo* peak isometric torque and fatigability) of the anterior crural muscles were performed as previously described[40-42]. Mice were anesthetize using isoflurane in O_2 with an isoflurane vaporizer. The left hindlimb was shaved, and betadine and ethanol pads were utilized to clean the skin. The animals were placed in a supine position in an Aurora Dual-Mode Lever System (Model 300B-LR, Aurora Scientific, Ontario, Canada). A heating pat was utilized to maintain their body temperature at 37°C. The left knee was positioned at a 90° angle to the foot, and the leg perpendicular to the

force pedal. The animal's foot was attached and secured to the footplate with the heel set in the groove and the toes firmly planted. Two needle electrodes (Model E2–12, Grass Technologies, West Warwick, RI, USA) were subcutaneously placed on the left common peroneal nerve within less than one mm apart. Twitch contractions were monitored in real-time using the Dynamic Muscle Control and Analysis (DMC) Software (615A, Aurora Scientific Inc., Ontario, Canada). An initial stimulus was measured at 150 Hz to ensure the electrodes were neither too deep nor too proximal to cause recruitment of the posterior crural muscle. After resting the hindlimb for one minute, torque and M-wave as a function of stimulation (torque) frequency were measured during 12 isometric contractions with the duration of 150 ms at various stimulation frequencies (10, 20, 30, 40, 60, 80, 100, 125, 150, 200, 250, and 300 Hz) to determine hindlimb motor unit recruitment. After four minutes of resting, 120 stimuli (one stimuli/second) were generated at 40 Hz to measure fatigability. After 10 minutes of rest, a recovery stimulus was measured using the same parameter for the initial stimulus. After the fatigability test, the normal movement of experimental mice was closely monitored to determine any injuries during the *in vivo* muscle contractility test. Torque (mN•m) was normalized by tumor free-body weight to account for differences in body size among experimental mice. Fatigability was calculated as a percentage from the peak force production. All data were analyzed using the Dynamic Muscle Data Acquisition and Analysis System (605A, Aurora Scientific Inc., Ontario, Canada).

2.4 Harvest and Tissue Collection

After 10, 15, 20, or 25 days from the C26 cancer injections, mice were deeply anesthetized with isoflurane in O_2. Soleus, tibialis anterior (TA), and gastrocnemius muscles were collected by tissue dissection and weighted using an analytic scale. Tumors, spleen, and fat were collected

and weighted using an analytic scale. Mice were immediately euthanized following tissue collection. Tibia was removed and measured using a caliper as a surrogate measure of total body size. Tissues weights were expressed normalized to tibia length. Tissues were immediately put on liquid nitrogen after collection and further storage at -80°C until RNA extraction.

2.5 RNA Isolation

Briefly, RNA was isolated using a commercially available kit (K145002, Invitrogen, Carlsbad, CA, USA), as described[40,41]. Tissues were powdered using a stainless-steel tissue cryopulverizer. 15-20 mg of frozen powdered tissue were suspended in one mL of cold TRIzol (10296-028, Invitrogen, Carlsbad, CA, USA) and homogenized using polytron for ~five seconds x four times or until tissue was completely homogenized. Homogenization solution was transferred to a 1.5 mL Eppendorf tube and allowed to sit for 15 minutes at room temperature. Organic phase separation was induced by adding 200 mL of 100% chloroform and then shaken vigorously for 15 seconds. After three minutes at room temperature, tubes were centrifuged 25 minutes at 15,000 rpm at 4°C until layers were separated. 400-700 uL of the top clear layer were transferred to a new sterile tube, and an equal amount of 70% diethyl pyrocarbonate (DEPC) ethanol was added to help RNA precipitation. Solution was transferred to a RNeasy column and spun 30 seconds at 8,070 rpm. Filtered flow was discarded, and 700 uL of Wash Buffer I added into column. Tubes were spun 15 seconds at 10,000 rpm. Column was transferred to a new collection tube, and 500 uL of Wash Buffer II was added. Samples were spun 15 seconds at 10,000 rpm. After one minute at room temperature, they were dried by spinning once again for one minute at 10,000 rpm. 20 uL of RNase free water was added into the column, and a new

recovery tube was placed. After one minute at room temperature, RNA samples were eluted after spinning for one minute at 10,000 rpm. A 260/280 nm radio > 1.8 was measured for RNA concentrations using Take3 micro-volume plate reader and gen5 software (BioTek Instruments, VT, USA). RNA samples were stored at -80°C until further use.

2.6 cDNA Synthesis

cDNA was synthesized by reverse transcription using four uL of cDNA SuperScript VILO Master Mix (11755500, Thermofisher Scientific, USA) and one ug/uL of RNA sample as described before [40,41]. The final solution was filled with sterile filtered deionized water (ddH2O) to a final volume of 20 uL per sample. Thermocycler was set for 25°C for 10 minutes, 42°C for 50 minutes, and 70°C for 15 minutes. 1:100 dilutions with ddH_2O were made and stored at -20°C until further use for RT-PCR.

2.7 Real-Time Quantitative PCR (RT-PCR)

cDNA quantification through cycle threshold (C_T) was measured using QuantStudio 3 Real-Time PCR system (Applied Biosystems, MA, USA). PCR reaction mix for TaqMan probes was prepared with 10X TaqMan™ Fast Advanced Master Mix (Applied Biosystems, 4444558), 1X of TaqMan™ Gene Expression Assay (FAM) (Applied Biosystems, 4331182), 1X of ddH_2O, and 8X of cDNA 1:100 dilution sample, to attain a 25 uL final volume reaction, as previously done[41]. The amplification protocol required an incubation time of two minutes at 50°C and 95°C for 10 minutes, followed by 45 cycles of denaturation at 95°C for 15 seconds, and annealing and

extension at 60°C for one minute. *Fis1* C_T value was measured using a SYBR green PCR probe. Primers were designed as described before by Greene and collaborators[41]. PCR reaction mix was prepared with 10X Power SYBR™ Green PCR Master Mix (Applied Biosystems, 4367659), 1X of reverse primmer 1:10 dilution (primer sequence AACCAGGCACCAGGCATATT), 1X of forward primmer 1:10 dilution (primer sequence ACGAAGCTGCAAGGAATTTTGA), and 8X of cDNA 1:100 dilution sample, to attain a 25 uL final volume reaction. Following the previously described amplification protocol. *18s* probe (Applied Biosystems, ID Mm03928990_g1) was used to measure each sample's *18s* RNA gene expression as housekeeping gene reaction. The ΔC_T values for each sample were calculated as the difference between the targeted gene C_T value and *18s* RNA C_T value (target – *18s*). Final quantification of gene expression was estimated using the ΔΔCT method. ΔΔCT values were calculated by the difference between the sample ΔCT and the average of group's ΔCT (ΔCT – Average of ΔCT). Relative quantification was calculated as $2^{-\Delta\Delta CT}$ as previously described [1]. The fluoresce-label probes used in this study were the following: *Fis1*, *Opa1* (Applied Biosystems, ID Mm01349707_g1), *Bnip3* (Applied Biosystems, ID Mm01275600_g1), *Lonp1* (Applied Biosystems, ID Mm01236887_m1), and *Parl1* (Applied Biosystems, ID Mm01343688_m1). All targets were normalized to the *18s* C_T value, which did not differ between groups. Corrected-final fold change for each group was reported as the relationship between each group's fold change and the average fold change from PBS/Control group.

2.8 Statistics

Statistical analyses were completed using GraphPad Prism 9 statistical software. All data are presented as means ± standard error of the mean (*M* ± *SEM*). Outlier values were excluded if

exceeded ± two standard deviations (SD). A one-way analysis of variation (ANOVA) was utilized as the global analysis for all variables to identify differences between groups. When significant F ratios were found, differences among means were determined using Tukey's post hoc test. For all statistical tests, α was set at 0.05.

3. Results

Table 1. Body and Tissue Weights at the Time of Harvest in C26 Tumor-Bearing Mice

Group	PBS ± SEM (n= 13)	10 Day ± SEM (n= 11)	15 Day ± SEM (n= 11)	20 Day ± SEM (n= 14)	25 Day ± SEM (n= 20)
Body Weight (g/mm)	1.662 ± 0.023 a	1.630 ± 0.028 ab	1.735 ± 0.025 a	1.661 ± 0.034 a	1.540 ± 0.022 b
Tumor Weight (g/mm)	N/A	0.018 ±0.005 a	0.150 ± 0.024 b	1.169 ± 0.130 b	2.360 ± 0.183 b
Tumor Free Body Weight (g/mm)	1.662 ± 0.023 ab	1.629 ± 0.028 ab	1.706 ± 0.021 a	1.585 ± 0.033 b	1.411 ± 0.025 c
Soleus (mg/mm)	0.541 ± 0.017 ab	0.546 ± 0.015 ab	0.583 ± 0.021 a	0.502 ± 0.019 ab	0.490 ± 0.012 b
Gastrocnemius (mg/mm)	8.478 ± 0.143 a	8.072 ± 0.203 a	8.573 ± 0.195 a	8.053 ± 0.183 a	7.053 ± 0.168 b
TA (mg/mm)	2.851 ± 0.037 a	2.650 ± 0.068 a	2.670 ± 0.057 a	2.675 ± 0.058 a	2.298 ± 0.066 b
Spleen (mg/mm)	5.628 ± 0.132 a	6.079 ± 0.131 a	6.444 ± 0.241 a	10.501 ± 0.475 b	14.372 ± 0.581 c
Gonadal fat (mg/mm)	27.647 ± 1.062 a	24.123 ±1.382 a	25.421 ± 1.320 a	21.318 ± 1.053 b	14.039 ± 1.533 b
Tibia Length (mm)	16.481 ± 0.070 a	15.932 ± 0.174 ab	15.534 ± 0.146 b	15.852 ± 0.224 abc	16.238 ± 0.126 ac

Table 1. Body and tissue weights were normalized by the tibia length. Values are presented as the mean ± SEM; abc denotes significative differences between groups, and n represents the number of animals in each group.

3.1 Colorectal-Cancer induce Cachexia in Tumor-Bearing Male Mice

Despite an increase in tumor size, 25 days after cancer injections, body weight and tumor-free body weight (TFBW) were 7.34% ($p=0.0074$) and 15.1% ($p<0.0001$) lower respectively, than PBS control. At the 25-day time point, soleus, gastrocnemius, and TA muscles weights were 9.43%, 16.81% ($p<0.0001$), and 19.4% ($p<0.0001$) lower compared to PBS group, respectively. Tumor-bearing mice had 49.22% ($p<0.0001$) lower fat content in the 25-day group and 22.89% ($p=0.0165$) in the 20-day group when compared with PBS control. Spleen weight was significantly greater after 20 (86.5%, $p<0.0001$) and 25 days (155.3%, $p<0.0001$) following tumor implantation compared to PBS control (Table 1).

3.2 *In Vivo* Assessment of Muscle Function

Skeletal muscle contractility was measured by *in vivo* peak isometric torque to estimate the muscular force response of each of the groups. 10-day group was 28.99% ($p=0.0377$) lower at 60 Hz, 22.72% ($p=0.0240$) lower at 150 Hz, 23.01% ($p=0.0404$) lower at 200 Hz, and 24.24% ($p=0.0459$) lower at 250 Hz, when compared with PBS control. 25-day group was 19.67% ($p=0.0913$) lower at 150 Hz; 28.40% ($p=0.0116$) lower at 200 Hz; 32.73% ($p=0.0459$) lower at 250 Hz; and 32.82% ($p=0.0046$) lower than control at 300 Hz. 10-day group was 36.99% ($p=0.0223$) lower at 30 Hz from the 15-day group (Figure 1A). When torque frequency was normalized by TFBW, while not always statistically significant the major differences were observed at lower frequencies (Figure 1B). 10-day group force was lower than 15-day group force at 20 Hz (27.36%, $p=0.0697$), at 30 Hz (33.07%, $p=0.0223$), and at 40 Hz (31.33%, $p=0.0890$). 10-day group force was also lower than 25-day group at 20 Hz (25.50%, $p=0.0958$), 40 Hz (34.27%, $p=0.0116$), and 60 Hz (28.26%, $p=0.0108$). No differences against control were

observed after normalization. The fatigability test revealed no statistical difference between PBS and 25-day group. However, 25-day group had 34.20% and 12.15% higher mean fatigability at 60 and 70 seconds respectively, after peak torque was achieved. Moreover, PBS control had ~27-30% lower fatigability (higher % peak torque) than 10-day group after 20, 30, and 40 seconds after the peak force ($p<0.05$). 25-day group had ~29-35% and ~27-30% higher fatigability (lower % peak torque), between 10-60 seconds after the maximum, than 10-day and 15-day groups, respectively ($p<0.05$) (Figure 1C).

3.3 Canonical Mitochondrial Quality Control Markers

Opa1 and *Fis1* mRNA contents were measured in soleus, gastrocnemius, and TA muscles to evaluate regulators of mitochondrial dynamics. *Opa1* was 27.3% ($p=0.053$) lower than control in soleus muscle after 10 days of cancer injections, with no significant difference observed after 25 days (Figure 2A). *Opa1* mRNA content was lower in the 25-days gastrocnemius by 13.7% ($p=0.1953$) and in TA by 26.3% ($p<0.0001$) when compared against PBS control (Figure 2B-C). When comparing 10-day against 25-day groups, 25.1% ($p=0.022$) and 17.2% ($p=0.0110$) lower contents were observed in gastrocnemius and TA muscles for *Opa1* content, respectively. *Fis1* mRNA content in soleus muscle was 34.0% ($p<0.0001$), 18.3% ($p=0.0229$), lower in 15-day and 20-day tumor-bearing groups compared to PBS control (Figure 2D). In gastrocnemius and TA muscle no significant difference in *Fis1* mRNA contents was observed in tumor-bearing groups compared to PBS control. After comparing *Fis1* expression, 20.8% ($p=0.0398$) in gastrocnemius and 22.3% in TA (mean difference not statistically significant, $p=0.0832$) lower content was observed in 25-day compared to 10-day tumor bearing (Figure 2E-F). *Bnip3* mRNA content was used as a marker to measure mitophagy. In soleus, *Bnip3* mRNA was 25.4% ($p=0.0395$) and

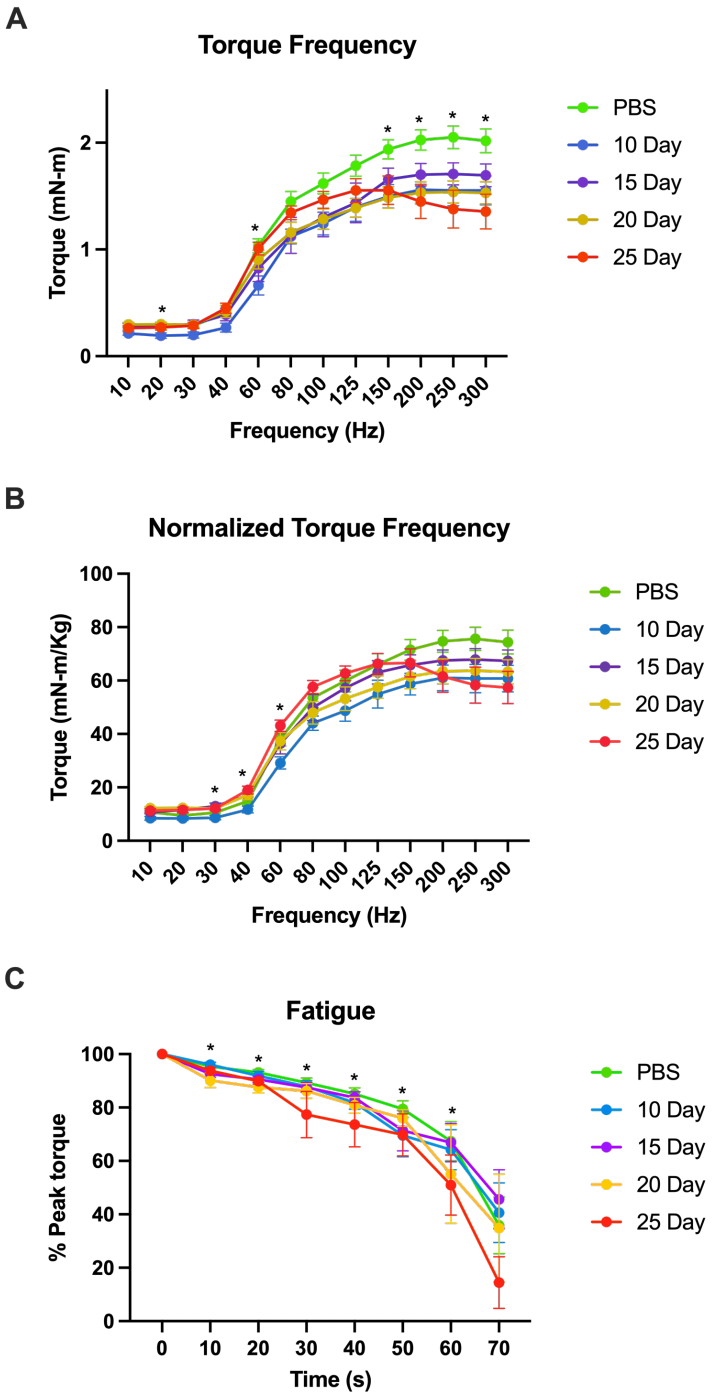

Figure 1. Torque Frequency and Fatigability. Torque and Fatigability of PBS group as control, and 10, 15, 20, or 25 days (d) groups after cancer injections. A. Torque Frequency in millinewtons/meter along 10-300 Hertz (Hz). B. Torque Frequency in millinewtons/meter along 10-300 Hertz (Hz), normalized by tumor-free body weight in kilograms (Kg). C. Fatigue analysis is shown each ten seconds per group as a percentage change from the peak (100%). * denotes significative differences among groups ($p<0.05$).

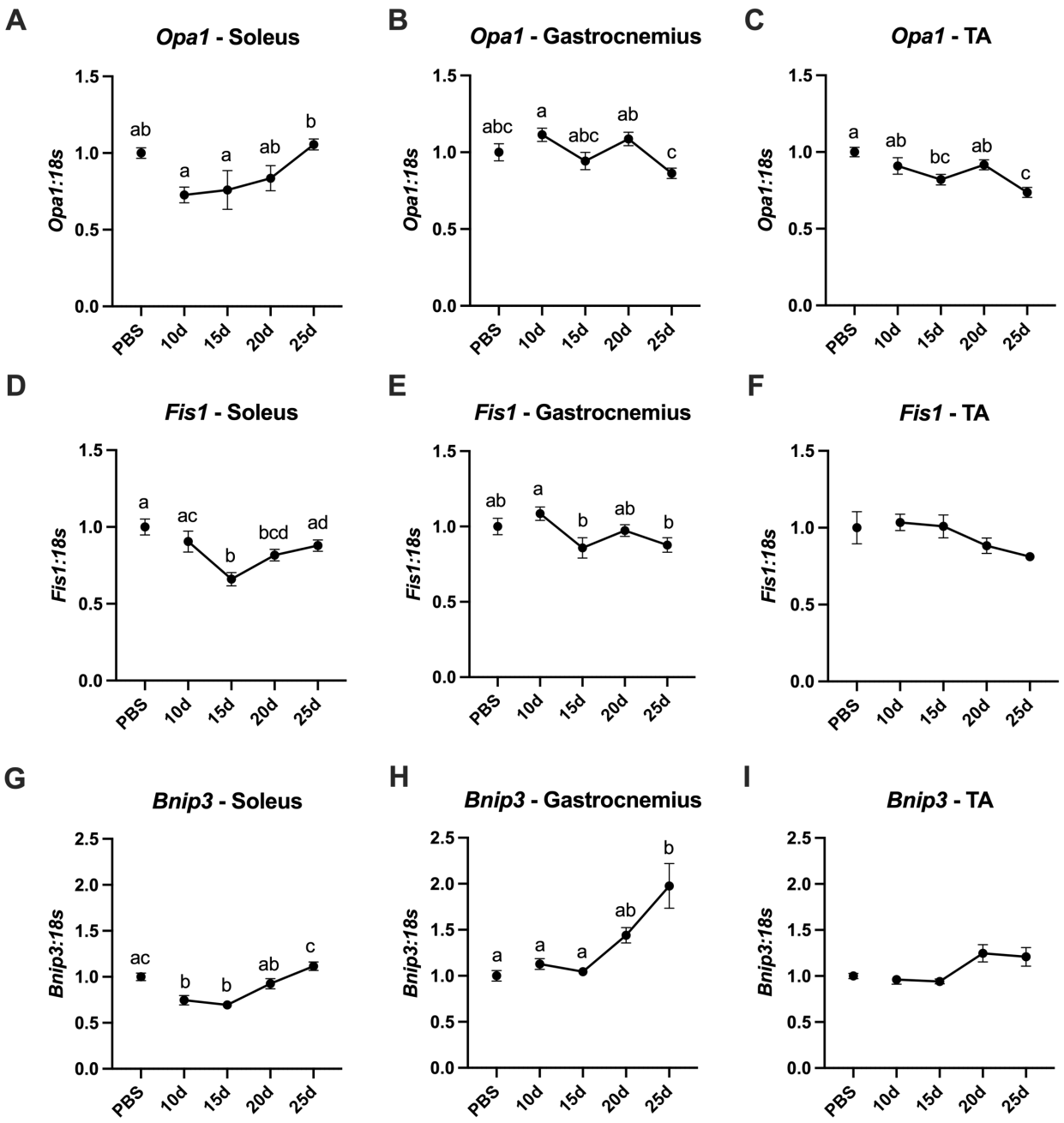

Figure 2. Mitochondrial Dynamics and Mitophagy. Quantification of gene expression estimated using the ΔΔCT method using *18s* RNA gene expression as normalization for abundancy in PBS group as control, and 10, 15, 20, or 25 days (d) groups after cancer injections. A. *Opa1* mRNA content in soleus muscle. B. *Opa1* mRNA content in gastrocnemius muscle. C. *Opa1* mRNA content in tiabilis anterior (TA) muscle. D. *Fis1* mRNA content in soleus muscle. E. *Fis1* mRNA content in gastrocnemius muscle. F. *Fis1* mRNA content in TA muscle. G. *Bnip3* mRNA content in soleus muscle. H. *Bnip3* mRNA content in gastrocnemius muscle. I. *Bnip3* mRNA content in TA muscle. Values are presented as the mean ± SEM; abc denotes significative differences between groups ($p<0.05$).

30.5% (p=0.0076) lower than PBS control in 10-day and 15-day groups, respectively; after 25 days of cancer injection (Figure 2G). In gastrocnemius 97.7% (p=0.0007) greater *Bnip3* content was observed in 25-day compared with control, with no significant differences in TA (Figure 2H-I).

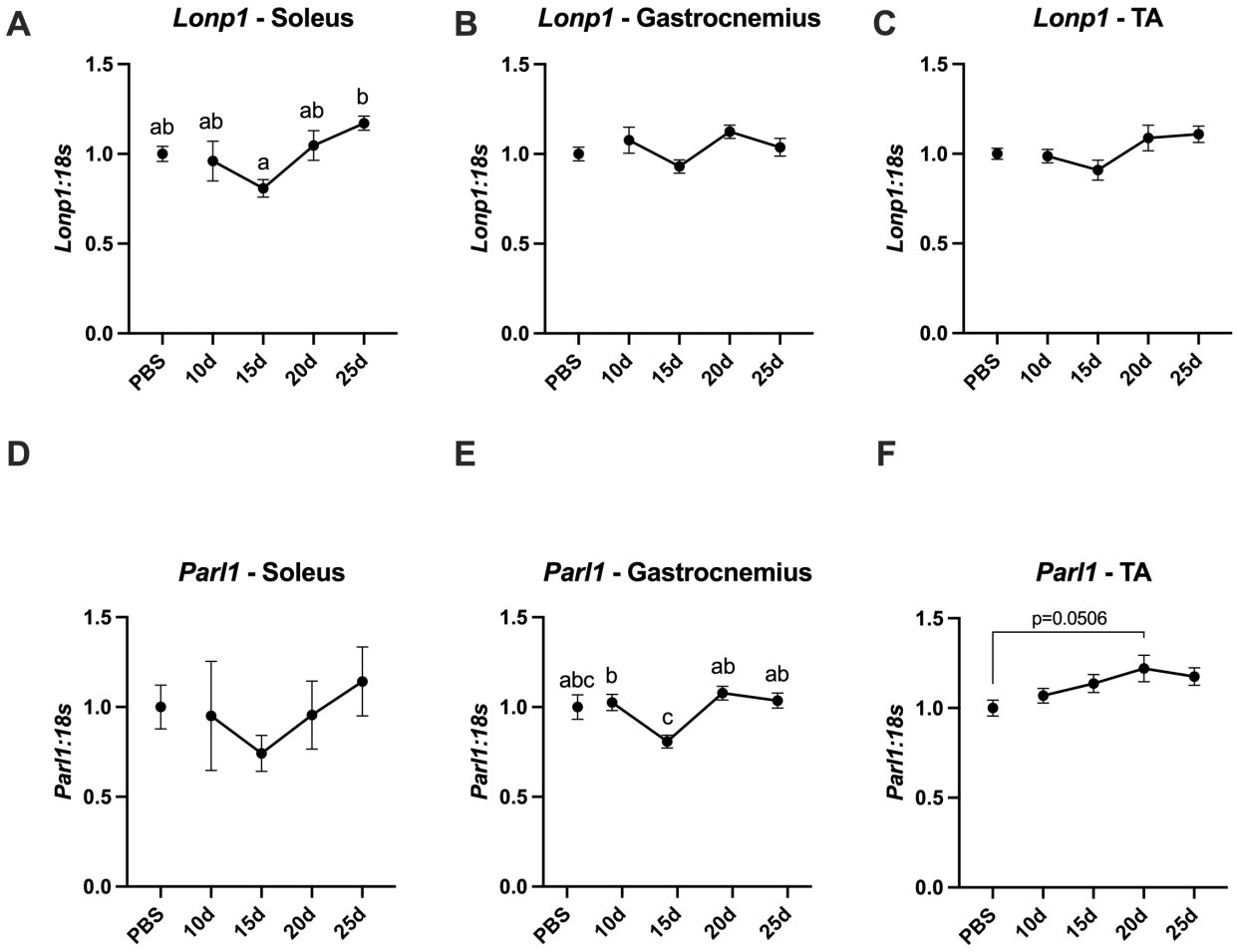

Figure 3. Mitochondrial Mitoproteases. Quantification of gene expression estimated using the ΔΔCT method using *18s* RNA gene expression as normalization for abundancy in PBS group as control, and 10, 15, 20, or 25 days (d) groups after cancer injections. A. *Lonp1* mRNA content in soleus muscle. B. *Lonp1* mRNA content in gastrocnemius muscle. C. *Lonp1* mRNA content in tiabilis anterior (TA) muscle. D. *Parl1* mRNA content in soleus muscle. E. *Parl1* mRNA content in gastrocnemius muscle. F. *Parl1* mRNA content in TA muscle. Values are presented as the mean ± SEM; abc denotes significative differences between groups ($p<0.05$).

3.4 Novel Mitochondrial Markers

Matrix mitochondrial - LONP1 and mitochondrial intermembrane space – PARL1 mitoproteases' mRNA content was measured. *Lonp1* mRNA content in soleus muscle was not different from PBS control in tumor-bearing groups, however, a 36.3% ($p=0.0120$) greater *Lonp1* mRNA was observed in 25-day compared to 15-day tumor-bearing groups (Figure 3A). No significant differences in *Lonp1* were observed in gastrocnemius or TA (Figure 3B-C). There was no difference in *Parl1* mRNA content in soleus muscle along the time-course (Figure 3D); for gastrocnemius 15-day group was 25-33% lower than other groups ($p<0.05$) (Figure 3E), and TA muscle 20-day group *Parl1* content was 22.1% higher than PBS control ($p=0.0506$) (Figure 3F).

4. Discussion

This study characterized contractile muscle functions and mitochondrial quality control changes in CC development using C26 colon carcinoma-induced male tumor-bearing mice. The major findings on this study were an overall reduction in muscular force with higher fatigue in the 25-day group and reduction in the expression of *Opa1* in TA muscle and increased expression of *Bnip3* on gastrocnemius.

The loss of muscle mass in CC emerges in response to catabolic stimuli leading to muscle wasting[8,42,43]. In this study, reduction in body mass started from day 10. This decrease remained along the time-course despite the increase in tumor weight (Table 1). The average tumor size obtained is in relation to what other studies that used C26 tumor transplants on BALB/c mice observed when a tumor growth kinetics was performed, they found a lag phase the first two weeks and a growth phase with tumors >larger than 2 g after 42 days of tumor implantation[44].

All tissue wet weights, including soleus, gastrocnemius, and tibialis anterior (TA), were measured at different time points after cancer injections (10, 15, 20, and 25 days). A progressive decrease in the mentioned tissues' weights can be observed from day 10 to day 25. This result is similar to other studies that used C26 as a CC model[45]. CC is mediated by the induction of cytokines (especially IL-6) by the spleen[46]. Splenomegaly was observed with a 250% increase in the spleen mass after 25 days of cancer injections. This value is similar to the 300% observed by Aulino and collaborators in their C26 transplant cachexia model[44]. But low when compared with the Lewis Lung Carcinoma (LLC) CC model previously done by our research group, in which a 4.5-fold increase in spleen mass was observed[1]. These varying degrees of cachexia can be due to different metabolic signals from the host, diverse cancer types, or tumor sizes[10]. Depletion of adipose tissue also contributes to the development of CC[47]. Adipose losses in this study were seen from day 10, becoming significative after 20 days, and with a waste up to 50% on day 25; similar to what Villars and collaborators found after 20 days using C26 tumor model[48].

As mentioned before, impaired muscle contractile function is associated with poor quality of life and serves as a predictor of survival for cancer patients[18-20]. In *vivo* muscle contractile function was assessed in anterior shin (crural) muscles to evaluate if weight and muscle loss impacted the absolute force. A significant decrease in peak isometric was noted 10 days following tumor allograft, especially at high frequencies (150-250 Hz). This reduction persisted after 25 days (Figure 1). When TFBW was utilized to normalize torque frequency, force was not different between tumor-bearing groups and PBS control mice. This finding is similar to previously reported by Aulino and collaborators using a C26 tumor-bearing mice model in BALB/c[44]. They found lower maximal force in Extensor digitorum longus (EDL) and soleus muscle that did not affect the specific force after normalization[44]. In the same way, Roberts and

collaborators found something similar in soleus muscle using C26 tumor-bearing mice model in CD2F1 mice[17]. In both studies, muscles were reported with reduced weights[17,44]. These findings suggest muscle weakness might be attributed to the decline in muscle mass more so than alterations in the intrinsic contractile properties of the myofibers[17,44]. Moreover, these findings highlight the heterogenicity of different muscle responses to CC[17,44]. When fatigability was investigated, major differences were observed between 10 and 15-day groups against control and 25-day group. Although there was no significant difference in fatigability test between the 25-day group and PBS control, in agreement with findings from Greenman and collaborators[49] in $APC^{Min/+}$ mice, 25-day group had ~12-34% higher fatigability than PBS control at the end of the trial.

Whereas altered mitochondrial health has been reported during CC, it is believed mitochondrial impairments might be the trigger event initiating cachexia-induced muscle loss[1,21]. In this study, *Opa1* and *Fis1* mRNA expression were measured along the 25-day time-course to characterize their levels during the onset of cachexia (Figure 2). The TA seems to be the tissue with the most significant reduction of *Opa1* expression after 25 days of cancer injections, where a 26.3% reduction was observed. Similarly, *Fis1* mRNA content was either slightly reduced or remained unchanged. Unbalanced mitochondrial dynamics can be deleterious, a compensatory mechanism of simultaneous reduction of fusion and fission processes has been proposed, whereby both processes are downregulated to mitigate detrimental effects induced by the loss of their homeostasis between these processes[14]. Prior study published by Huot and collaborators did not show alteration in OPA1or FIS1 protein levels using the C26 model on CD2F1 male mice after 15 days[50]. However, our laboratory previously demonstrated dysregulation in mitochondrial dynamics, reporting a reduction of ~ 45% reduction on OPA1 and ~80% induction

on FIS1 protein content in 4 weeks cachectic LLC tumor-bearing male mice[1]. These contrasts between mRNA, protein levels, and CC models reinforce the need for more detailed and deeper studies on cachexia that help understand tumor-host interactions, and any other variables may affect the onset and development of this condition. Furthermore, fragmented mitochondria have been associated with increased apoptosis [51]. This study observed a ~98% increase of *Bnip3* mRNA levels in gastrocnemius muscle after 25 days of cancer injections. Unpublished data from our research group has found a ~147% increase in *Bnip3* mRNA levels and ~63% increase in BNIP3 protein levels in LLC female mice[52]; furthermore, our laboratory has demonstrated dysregulation in mitophagy, reporting a ~ 200% increase of BNIP3 protein expressions in LLC tumor-bearing male mice[1]. These studies together, in addition with the findings in this study, show that BNIP3 is consistently elevated in gastrocnemius muscle of both sexes across forms of cancer, making this protein a tempting option as a CC therapeutic target.

Mitochondrial intrinsic protein turnover has recently been investigated as part of the MQC system [24,37]. A study conducted by Wagatsuma and collaborators demonstrated down-regulated LONP1 in hindlimb unloading (HU) induced disuse muscles in female CD1 mice[34,53]. Moreover, *Parl1*$^{-/-}$ mice have shown gradual muscle and organs atrophy, leading to cachexia-induced death in less than three months[54]. *Lonp1* and *Parl1* gene expression were used to provide insight into the status of this MQC component in the onset of CC. This study is the first to report these markers in a time-course C26 CC model to the best of my knowledge. Both *Lonp1* and *Parl1* mRNA content levels remained somewhat unchanged after the 25 days of the time-course. Both LONP1 and PARL1 have been shown to be evolutionarily conserved proteins with high importance for essential survival[34,54]. Even though their mRNA values are not affected during C26 CC evolution, their protein expression in this disease remains unknown.

In general, the measurement of muscular function and mitochondrial quality control markers in this study contributed to give a broader picture of the onset and behavior of CC along 25 days after cancer injections. Overall, this study demonstrated that colorectal cancer induces muscle wasting as fast as 10 days after the beginning of cancer. The muscle functionality here supports the theory that a decrease in muscle mass plays a vital role in reducing force enhancing muscle fatigability, while mitochondrial impairments vary along with the evolution of cachexia, potentially affecting the supply energy source for skeletal muscle to maintain muscle mass and function.

5. Conclusion

In conclusion, this study demonstrates that C26 induces skeletal muscle atrophy aggravated during development and progression. Higher fatigue is present after 25 days following tumor implantation, and an overall decrease in the isometric force can be seen starting after 10 days. These results reinforce the theory that muscle weakness can be attributed to the decline in muscle mass and may not be attributed to alterations in the intrinsic contractile properties of the myofibers. Further, a reduction in the expression of *Opa1* in TA muscle and increased expression of *Bnip3* on gastrocnemius was observed, pointing to intrinsic differences in mitochondrial metabolism and heterogenicity of different muscle responses to CC. This study was the first to report *Lonp1* and *Parl1* mRNA content in a time-course C26 CC model to the best of my knowledge. Even though no significant differences were found, it would be worth exploring how protein expression levels behave since studies have shown that mRNA levels do not perfectly align with their respective translated protein concentrations. All of the above underline the complexity of suggesting a model-mechanism for the onset and progression of CC along the

time-course of the disease that allows proposing therapeutic strategies to delay the start, diminish harshness or even prevent the disease.

6. Future Perspectives

This research focused on cancer-induced cachexia in male mice, it did not address variables such as biological sex. Different outcomes can be obtained by exploring sex differences in the variables to test. In addition, the results obtained in this study may contrast with results published elsewhere using different CC models or time points. For this reason, further investigation is needed addressing parameters such as sex, breeding, different muscles, organs, cancer type, or tumor sizes to fully characterize cachexia onset and develop.

7. Funding

This study was funded by the National Institute of Arthritis and Musculoskeletal and Skin Diseases of the National Institute of Health (NIH) awards R01AR075794-01A1/AR/NIAMS(NPG).

References

1 Brown, J. L. *et al.* Mitochondrial degeneration precedes the development of muscle atrophy in progression of cancer cachexia in tumour-bearing mice. *Journal of cachexia, sarcopenia and muscle* **8**, 926-938, doi:10.1002/jcsm.12232 (2017).

2 Amrute-Nayak, M. *et al.* Chemotherapy triggers cachexia by deregulating synergetic function of histone-modifying enzymes. *Journal of cachexia, sarcopenia and muscle* **12**, 159-176, doi:10.1002/jcsm.12645 (2021).

3 Fearon, K. P. *et al.* Definition and classification of cancer cachexia: an international consensus. *The lancet oncology* **12**, 489-495, doi:10.1016/S1470-2045(10)70218-7 (2011).

4 Siddiqui, J. A., Pothuraju, R., Jain, M., Batra, S. K. & Nasser, M. W. Advances in cancer cachexia: Intersection between affected organs, mediators, and pharmacological interventions. *Biochimica et biophysica acta. Reviews on cancer* **1873**, 188359-188359, doi:10.1016/j.bbcan.2020.188359 (2020).

5 Bielecka-Dabrowa, A. *et al.* Cachexia, muscle wasting, and frailty in cardiovascular disease. *European journal of heart failure* **22**, 2314-2326, doi:10.1002/ejhf.2011 (2020).

6 Ballarò, R. *et al.* Targeting Mitochondria by SS-31 Ameliorates the Whole Body Energy Status in Cancer- and Chemotherapy-Induced Cachexia. *Cancers* **13**, 850, doi:10.3390/cancers13040850 (2021).

7 van der Ende, M. *et al.* Mitochondrial dynamics in cancer-induced cachexia. *Biochimica et biophysica acta. Reviews on cancer* **1870**, 137-150, doi:10.1016/j.bbcan.2018.07.008 (2018).

8 Cohen, S., Nathan, J. A. & Goldberg, A. L. Muscle wasting in disease: molecular mechanisms and promising therapies. *Nature reviews. Drug discovery* **14**, 58-74, doi:10.1038/nrd4467 (2015).

9 Deval, C. *et al.* Mitophagy and Mitochondria Biogenesis Are Differentially Induced in Rat Skeletal Muscles during Immobilization and/or Remobilization. *International journal of molecular sciences* **21**, 3691, doi:10.3390/ijms21103691 (2020).

10 Rohm, M., Zeigerer, A., Machado, J. & Herzig, S. Energy metabolism in cachexia. *EMBO reports* **20**, n/a-n/a, doi:10.15252/embr.201847258 (2019).

11 Ding, W., Jiang, J., Xu, J., Cao, Y. & Xu, L. MURF contributes to skeletal muscle atrophy through suppressing autophagy. *International journal of clinical and experimental pathology U6 - ctx_ver=Z39.88-2004&ctx_enc=info%3Aofi%2Fenc%3AUTF-8&rfr_id=info%3Asid%2Fsummon.serialssolutions.com&rft_val_fmt=info%3Aofi%2Ffmt%3Akev%3Amtx%3Ajournal&rft.genre=article&rft.atitle=MURF+contributes+to+skeletal+muscle+atrophy+through+suppressing+autophagy&rft.jtitle=International+journal+of+clinical+and+experimental+pathology&rft.au=Ding%2C+Wei&rft.au=Jiang%2C+Junjian&rft.au=Xu%2C+Jianguang&rft.au=Cao%2C+Yu&rft.date=2017&rft.eissn=1936-2625&rft.volume=10&rft.issue=11&rft.spage=11075&rft_id=info%3Apmid%2F31966455&rft.externalDocID=31966455&paramdict=en-US U7 - Journal Article* **10**, 11075-11079 (2017).

12 Scicchitano, B. M., Dobrowolny, G., Sica, G. & Musaro, A. Molecular Insights into Muscle Homeostasis, Atrophy and Wasting. *Current genomics* **19**, 356-369, doi:10.2174/1389202919666180101153911 (2018).

13 Tisdale, M. J. Are tumoral factors responsible for host tissue wasting in cancer cachexia? *Future oncology (London, England)* **6**, 503-513, doi:10.2217/fon.10.20 (2010).

14 Romanello, V. & Sandri, M. The connection between the dynamic remodeling of the mitochondrial network and the regulation of muscle mass. *Cellular and molecular life sciences : CMLS* **78**, 1305-1328, doi:10.1007/s00018-020-03662-0 (2021).

15 Schmidt, S. F., Rohm, M., Herzig, S. & Diaz, M. B. Cancer Cachexia: More Than Skeletal Muscle Wasting. *Trends in cancer* **4**, 849-860, doi:10.1016/j.trecan.2018.10.001 (2018).

16 Jackson, K. M., Cole, C. L. & Dunne, R. F. From bench to bedside: updates in basic science, translational and clinical research on muscle fatigue in cancer cachexia. *Current opinion in clinical nutrition and metabolic care* **24**, 216-222, doi:10.1097/MCO.0000000000000738 (2021).

17 Roberts, B. M., Frye, G. S., Ahn, B., Ferreira, L. F. & Judge, A. R. Cancer cachexia decreases specific force and accelerates fatigue in limb muscle. *Biochemical and biophysical research communications* **435**, 488-492, doi:10.1016/j.bbrc.2013.05.018 (2013).

18 VanderVeen, B. N., Fix, D. K. & Carson, J. A. Disrupted Skeletal Muscle Mitochondrial Dynamics, Mitophagy, and Biogenesis during Cancer Cachexia: A Role for Inflammation. *Oxidative medicine and cellular longevity* **2017**, 3292087-3292013, doi:10.1155/2017/3292087 (2017).

19 Mehl, K. A. *et al.* Decreased intestinal polyp multiplicity is related to exercise mode and gender in ApcMin/+ mice. *Journal of Applied Physiology* **98**, 2219-2225, doi:10.1152/japplphysiol.00975.2004 (2005).

20 Kilgour, R. D. *et al.* Handgrip strength predicts survival and is associated with markers of clinical and functional outcomes in advanced cancer patients. *Supportive care in cancer* **21**, 3261-3270, doi:10.1007/s00520-013-1894-4 (2013).

21 Rosa-Caldwell, M. E., Fix, D. K., Washington, T. A. & Greene, N. P. Muscle alterations in the development and progression of cancer-induced muscle atrophy: a review. *Journal of applied physiology (1985)* **128**, 25-41, doi:10.1152/japplphysiol.00622.2019 (2020).

22 Penna, F., Ballarò, R. & Costelli, P. The Redox Balance: A Target for Interventions Against Muscle Wasting in Cancer Cachexia? *Antioxid Redox Signal* **33**, 542-558, doi:10.1089/ars.2020.8041 (2020).

23 Kiriyama, Y., Nochi, H., Yoshimitsu, K. & Hiromi, N. Intra- and Intercellular Quality Control Mechanisms of Mitochondria. *Cells (Basel, Switzerland)* **7**, 1, doi:10.3390/cells7010001 (2017).

24 Jadiya, P. & Tomar, D. Mitochondrial Protein Quality Control Mechanisms. *Genes* **11**, 563, doi:10.3390/genes11050563 (2020).

25 Carinci, M. *et al.* Different Roles of Mitochondria in Cell Death and Inflammation: Focusing on Mitochondrial Quality Control in Ischemic Stroke and Reperfusion. *Biomedicines* **9**, 169, doi:10.3390/biomedicines9020169 (2021).

26 Callegari, S. & Dennerlein, S. Sensing the Stress: A Role for the UPRmt and UPRam in the Quality Control of Mitochondria. *Frontiers in cell and developmental biology* **6**, 31-31, doi:10.3389/fcell.2018.00031 (2018).

27 Romanello, V. & Sandri, M. Mitochondrial Quality Control and Muscle Mass Maintenance. *Frontiers in physiology* **6**, 422-422, doi:10.3389/fphys.2015.00422 (2015).

28 Mehrabani, S., Bagherniya, M., Askari, G., Read, M. I. & Sahebkar, A. The effect of fasting or calorie restriction on mitophagy induction: a literature review. *Journal of cachexia, sarcopenia and muscle* **11**, 1447-1458, doi:10.1002/jcsm.12611 (2020).

29 Cho, H. M. & Sun, W. Molecular cross talk among the components of the regulatory machinery of mitochondrial structure and quality control. *Experimental & molecular medicine* **52**, 730-737, doi:10.1038/s12276-020-0434-9 (2020).

30 Song, J., Herrmann, J. M. & Becker, T. Quality control of the mitochondrial proteome. *Nature reviews. Molecular cell biology U6 - ctx_ver=Z39.88-2004&ctx_enc=info%3Aofi%2Fenc%3AUTF-8&rfr_id=info%3Asid%2Fsummon.serialssolutions.com&rft_val_fmt=info%3Aofi%2Ffmt%3Akev%3Amtx%3Ajournal&rft.genre=article&rft.atitle=Quality+control+of+the+mitochondrial+proteome&rft.jtitle=Nature+reviews.+Molecular+cell+biology&rft.au=Song%2C+Jiyao&rft.au=Herrmann%2C+Johannes+M&rft.au=Becker%2C+Thomas&rft.date=2021-01-01&rft.eissn=1471-0080&rft.volume=22&rft.issue=1&rft.spage=54&rft_id=info%3Apmid%2F33093673&rft_id=info%3Apmid%2F33093673&rft.externalDocID=33093673&paramdict=en-US U7 - Journal Article* **22**, 54 (2021).

31 Fix, D. K., VanderVeen, B. N., Counts, B. R. & Carson, J. A. Regulation of Skeletal Muscle DRP-1 and FIS-1 Protein Expression by IL-6 Signaling. *Oxidative medicine and cellular longevity* **2019**, 8908457-8908412, doi:10.1155/2019/8908457 (2019).

32 Vernucci, E. *et al.* Mitophagy and Oxidative Stress in Cancer and Aging: Focus on Sirtuins and Nanomaterials. *Oxidative medicine and cellular longevity* **2019**, 6387357-6387319, doi:10.1155/2019/6387357 (2019).

33 Goard, C. A. & Schimmer, A. D. Mitochondrial matrix proteases as novel therapeutic targets in malignancy. *Oncogene* **33**, 2690-2699, doi:10.1038/onc.2013.228 (2014).

34 Bota, D. A. & Davies, K. J. A. Mitochondrial Lon protease in human disease and aging: Including an etiologic classification of Lon-related diseases and disorders. *Free radical biology & medicine* **100**, 188-198, doi:10.1016/j.freeradbiomed.2016.06.031 (2016).

35 Ghosh, R., Vinod, V., Symons, J. D. & Boudina, S. Protein and Mitochondria Quality Control Mechanisms and Cardiac Aging. *Cells (Basel, Switzerland)* **9**, 933, doi:10.3390/cells9040933 (2020).

36 Venkatesh, S. & Suzuki, C. K. Cell stress management by the mitochondrial LonP1 protease - Insights into mitigating developmental, oncogenic and cardiac stress. *Mitochondrion U6 - ctx_ver=Z39.88-2004&ctx_enc=info%3Aofi%2Fenc%3AUTF-8&rfr_id=info%3Asid%2Fsummon.serialssolutions.com&rft_val_fmt=info%3Aofi%2Ffmt%3Akev%3Amtx%3Ajournal&rft.genre=article&rft.atitle=Cell+stress+management+by+the+mitochondrial+LonP1+protease+-*

+Insights+into+mitigating+developmental%2C+oncogenic+and+cardiac+stress&rft.jtitle=Mitochondrion&rft.au=Venkatesh%2C+Sundararajan&rft.au=Suzuki%2C+Carolyn+K&rft.date=2020-03-01&rft.eissn=1872-8278&rft.volume=51&rft.spage=46&rft_id=info%3Apmid%2F31756517&rft_id=info%3Apmid%2F31756517&rft.externalDocID=31756517&paramdict=en-US U7 - Journal Article **51**, 46 (2020).

37 Huang, S. *et al.* LonP1 regulates mitochondrial network remodeling through the PINK1/Parkin pathway during myoblast differentiation. *American Journal of Physiology: Cell Physiology* **319**, C1020-C1028, doi:10.1152/ajpcell.00589.2019 (2020).

38 Gibellini, L. *et al.* The biology of Lonp1: More than a mitochondrial protease. *International review of cell and molecular biology* **354**, 1 (2020).

39 Lysyk, L., Brassard, R., Touret, N. & Lemieux, M. J. PARL Protease: A Glimpse at Intramembrane Proteolysis in the Inner Mitochondrial Membrane. *Journal of molecular biology* **432**, 5052-5062, doi:10.1016/j.jmb.2020.04.006 (2020).

40 Rosa-Caldwell, M. E. *et al.* Female mice may have exacerbated catabolic signalling response compared to male mice during development and progression of disuse atrophy. *Journal of cachexia, sarcopenia and muscle* **12**, 717-730, doi:10.1002/jcsm.12693 (2021).

41 Greene, N. P. *et al.* Mitochondrial quality control, promoted by PGC-1α, is dysregulated by Western diet-induced obesity and partially restored by moderate physical activity in mice. *Physiological reports* **3**, e12470-n/a, doi:10.14814/phy2.12470 (2015).

42 Fanzani, A., Conraads, V. M., Penna, F. & Martinet, W. Molecular and cellular mechanisms of skeletal muscle atrophy: an update. *Journal of cachexia, sarcopenia and muscle* **3**, 163-179, doi:10.1007/s13539-012-0074-6 (2012).

43 McKinnell, I. W. & Rudnicki, M. A. Vol. 119 907-910 (Elsevier Inc, United States, 2004).

44 Aulino, P. *et al.* Molecular, cellular and physiological characterization of the cancer cachexia-inducing C26 colon carcinoma in mouse. *BMC cancer* **10**, 363-363, doi:10.1186/1471-2407-10-363 (2010).

45 Murphy, K. T., Chee, A., Trieu, J., Naim, T. & Lynch, G. S. Importance of functional and metabolic impairments in the characterization of the C-26 murine model of cancer cachexia. *Disease models & mechanisms* **5**, 533-545, doi:10.1242/dmm.008839 (2012).

46 Barton, B. E. & Murphy, T. F. CANCER CACHEXIA IS MEDIATED IN PART BY THE INDUCTION OF IL-6-LIKE CYTOKINES FROM THE SPLEEN. *Cytokine (Philadelphia, Pa.)* **16**, 251-257, doi:10.1006/cyto.2001.0968 (2001).

47 Han, J., Meng, Q., Shen, L. & Wu, G. Interleukin-6 induces fat loss in cancer cachexia by promoting white adipose tissue lipolysis and browning. *Lipids in health and disease* **17**, 14-14, doi:10.1186/s12944-018-0657-0 (2018).

48 Villars, F. O., Pietra, C., Giuliano, C., Lutz, T. A. & Riediger, T. Oral Treatment with the Ghrelin Receptor Agonist HM01 Attenuates Cachexia in Mice Bearing Colon-26 (C26) Tumors. *International journal of molecular sciences* **18**, 986, doi:10.3390/ijms18050986 (2017).

49 Greenman, A. C., Albrecht, D. M., Halberg, R. B. & Diffee, G. M. Sex differences in skeletal muscle alterations in a model of colorectal cancer. *Physiological reports U6 - ctx_ver=Z39.88-2004&ctx_enc=info%3Aofi%2Fenc%3AUTF-8&rfr_id=info%3Asid%2Fsummon.serialssolutions.com&rft_val_fmt=info%3Aofi%2Ffmt%3Akev%3Amtx%3Ajournal&rft.genre=article&rft.atitle=Sex+differences+in+skeletal+muscle+alterations+in+a+model+of+colorectal+cancer&rft.jtitle=Physiological+reports&rft.au=Greenman%2C+Angela+C&rft.au=Albrecht%2C+Dawn+M&rft.au=Halberg%2C+Richard+B&rft.au=Diffee%2C+Gary+M&rft.date=2020-03-01&rft.eissn=2051-817X&rft.volume=8&rft.issue=5&rft.epage=n%2Fa&rft_id=info:doi/10.14814%2Fphy2.14391&rft.externalDocID=PHY214391&paramdict=en-US U7 - Journal Article* **8**, e14391-n/a, doi:10.14814/phy2.14391 (2020).

50 Huot, J. R. *et al.* Formation of colorectal liver metastases induces musculoskeletal and metabolic abnormalities consistent with exacerbated cachexia. *JCI insight* **5**, doi:10.1172/jci.insight.136687 (2020).

51 Szabo, A. *et al.* Activation of mitochondrial fusion provides a new treatment for mitochondria-related diseases. *Biochemical pharmacology* **150**, 86-96, doi:10.1016/j.bcp.2018.01.038 (2018).

52 Lim, S., Deaver, J., Rosa-Caldwell, M., et & al. Time-course of metabolic and contractile alterations in development of cancer cachexia in female tumor-bearing mice. *Summited in j Cachexia Sarcopenia Muscle* (June 5, 2021).

53 Wagatsuma, A. *et al.* Mitochondrial adaptations in skeletal muscle to hindlimb unloading. *Molecular and cellular biochemistry* **350**, 1-11, doi:10.1007/s11010-010-0677-1 (2011).

54 Cipolat, S. *et al.* Mitochondrial Rhomboid PARL Regulates Cytochrome c Release during Apoptosis via OPA1-Dependent Cristae Remodeling. *Cell* **126**, 163-175, doi:10.1016/j.cell.2006.06.021 (2006).

Appendix

Figure S.1 Research Protocol Approval - Institutional Biosafety Committee (IBC number 20009)

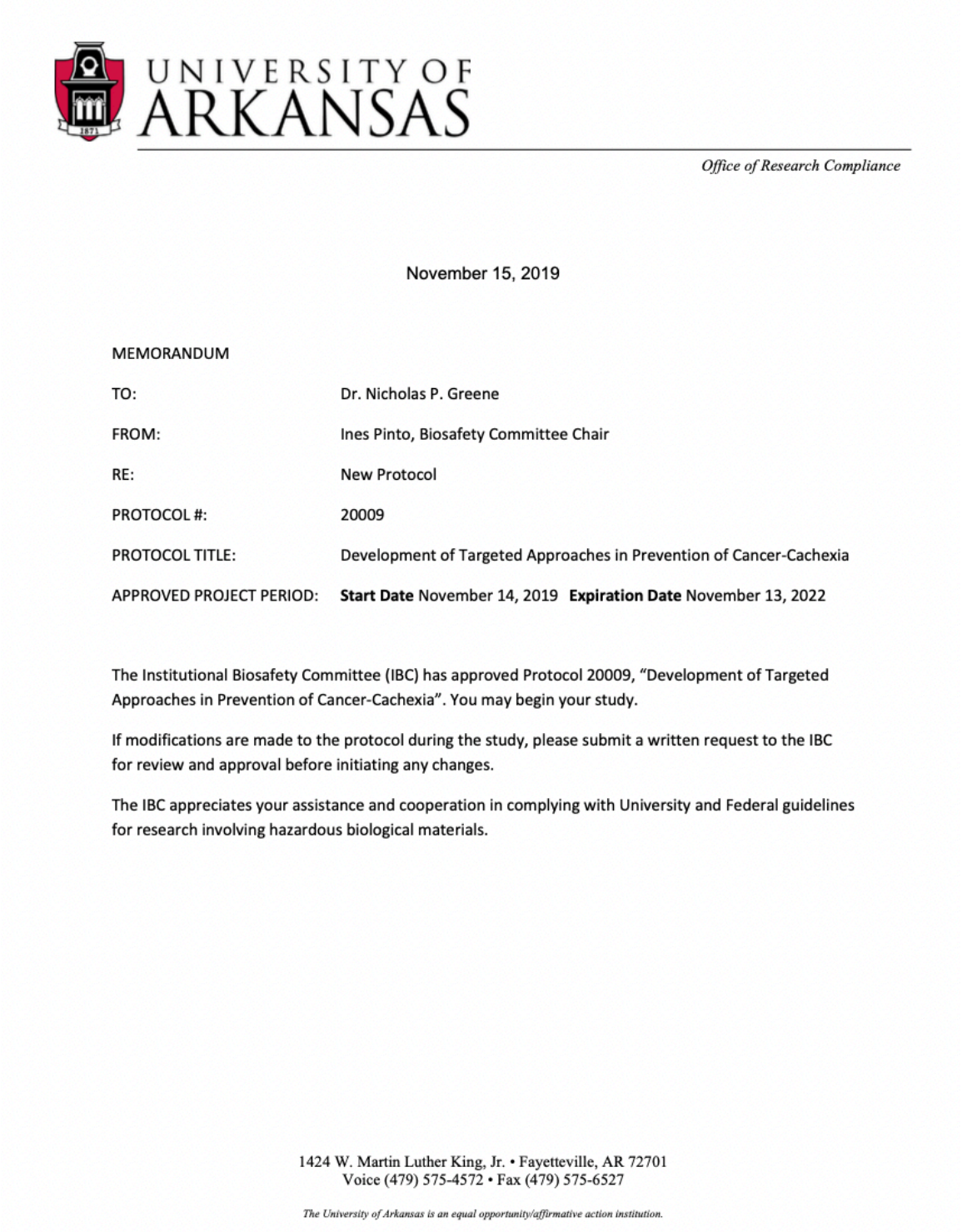

UNIVERSITY OF ARKANSAS

Office of Research Compliance

November 15, 2019

MEMORANDUM

TO:	Dr. Nicholas P. Greene
FROM:	Ines Pinto, Biosafety Committee Chair
RE:	New Protocol
PROTOCOL #:	20009
PROTOCOL TITLE:	Development of Targeted Approaches in Prevention of Cancer-Cachexia
APPROVED PROJECT PERIOD:	**Start Date** November 14, 2019 **Expiration Date** November 13, 2022

The Institutional Biosafety Committee (IBC) has approved Protocol 20009, "Development of Targeted Approaches in Prevention of Cancer-Cachexia". You may begin your study.

If modifications are made to the protocol during the study, please submit a written request to the IBC for review and approval before initiating any changes.

The IBC appreciates your assistance and cooperation in complying with University and Federal guidelines for research involving hazardous biological materials.

1424 W. Martin Luther King, Jr. • Fayetteville, AR 72701
Voice (479) 575-4572 • Fax (479) 575-6527

The University of Arkansas is an equal opportunity/affirmative action institution.

Figure S.2 Research Protocol Approval - Institutional Animal Care and Use Committees of the University of Arkansas -IACUC (Animal Use Protocol (AUP) number 20041).

UNIVERSITY OF ARKANSAS

Office of Research Compliance

To: Nicholas Greene
From: Jeff Wolchok
Date: November 25, 2019
Subject: IACUC Approval
Expiration Date: November 24, 2022

The Institutional Animal Care and Use Committee (IACUC) has APPROVED your protocol #**20041**, *Aim 1.1.1, Development of cancer-induced muscle loss during development of C26 induced colorectal cancer*.

In granting its approval, the IACUC has approved only the information provided. Should there by any further changes to the protocol during the research, please notify the IACUC in writing (via the Modification form) prior to initiating the changes. If the study period is expected to extend beyond November 24, 2022 you may submit a modification to extend the project up to three years, or submit a new protocol. The IACUC may not approve a study for more than three years at a time.

The following individuals are approved to work on this study: Nicholas Greene, Tyrone Washington, Seongkyun Lim, and Wesley Haynie. Please submit personnel additions to this protocol via the modification form prior to their starting work.

The IACUC appreciates your cooperation in complying with University and federal guidelines involving the care and use of animals.

JCW/jgr

1424 W. Martin Luther King, Jr. • Fayetteville, AR 72701
Voice (479) 575-4572 • Fax (479) 575-6527

Figure S.3 Letter of Approval

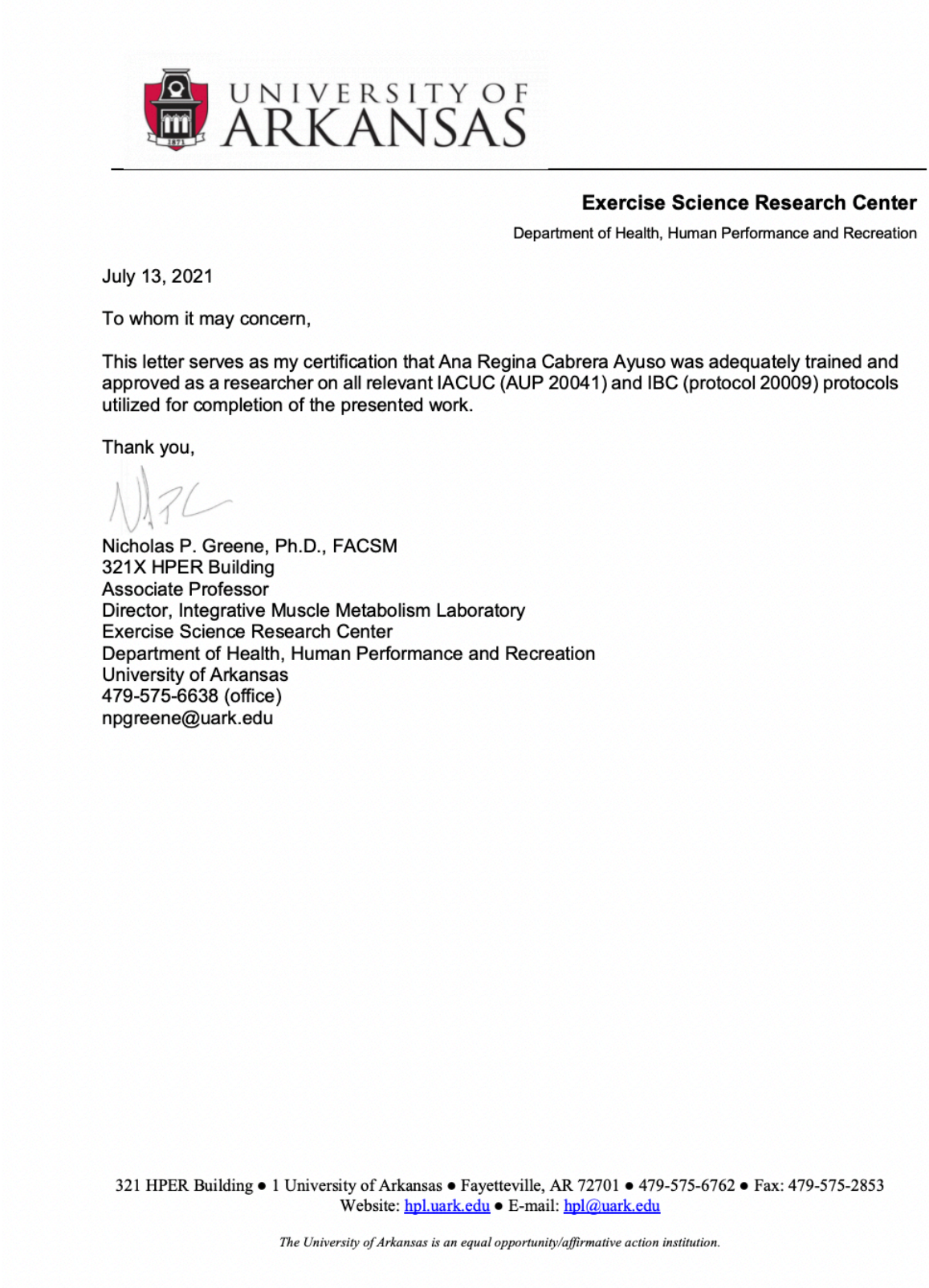

UNIVERSITY OF ARKANSAS

Exercise Science Research Center

Department of Health, Human Performance and Recreation

July 13, 2021

To whom it may concern,

This letter serves as my certification that Ana Regina Cabrera Ayuso was adequately trained and approved as a researcher on all relevant IACUC (AUP 20041) and IBC (protocol 20009) protocols utilized for completion of the presented work.

Thank you,

Nicholas P. Greene, Ph.D., FACSM
321X HPER Building
Associate Professor
Director, Integrative Muscle Metabolism Laboratory
Exercise Science Research Center
Department of Health, Human Performance and Recreation
University of Arkansas
479-575-6638 (office)
npgreene@uark.edu

321 HPER Building ● 1 University of Arkansas ● Fayetteville, AR 72701 ● 479-575-6762 ● Fax: 479-575-2853
Website: hpl.uark.edu ● E-mail: hpl@uark.edu

The University of Arkansas is an equal opportunity/affirmative action institution.